$= 2$) was designed with $Q = 0$, $R = 0.1$ in Eq. (14). The parameters k_i were adjusted to achieve the desired damping in the structural modes.

Experience with the solution procedure showed that the damping on the closed-loop structural modes could be individually adjusted by the choice of k_i. Moreover, the damping can be introduced with only minor change in natural frequency. Figure 1 illustrates the effect that increasing k_1 has on the modal damping, with $k_2 = 0$. Note that this results in increased damping on the first mode, whereas the second mode remains relatively unaffected. Figure 2 illustrates the fact that increasing k_2 with $k_1 = 0$ has the opposite effect. In both cases, the compensator introduces two additional closed-loop, low-frequency poles that are almost unobservable in the plant states.

For $k_1 = 350$, $k_2 = 345$, the closed-loop structural mode dampings were $\zeta_1 = 0.52$ and $\zeta_2 = 0.70$, respectively. Attempts to increase the damping further resulted in convergence difficulties with the numerical algorithm used to find the optimal G. Normally, the algorithm converged in fewer than 10 iterations.

The final solution was

$$G = \left[\begin{array}{cc|c} -54.3 & -628.5 & 0.687 \\ -922.0 & -1.19 \times 10^6 & 126.8 \end{array}\right] \qquad (22)$$

Conclusions

A method for designing fixed-order compensators using frequency-shaped cost functionals has been outlined. The major advantages are that the order of the compensator is fixed by the design process, and it is not necessary to realize the frequency-shaping dynamics as an integral part of the compensator design. The example illustrates the use of the design procedure to damp the fast structural modes of a flexible arm.

Acknowledgment

This research was supported by NASA Langley Research Center under Grant NAG-1-283.

References

[1]Gupta, N. K., "Frequency-Shaped Cost Functionals: Extensions of Linear Quadratic-Gaussian Design Methods," *Journal of Guidance and Control,* Vol. 3, Nov.-Dec. 1980, pp. 529-535.

[2]Anderson, B. D. O. and Mingori, D. L., "Use of Frequency Dependence in Linear Quadratic Control Problems to Frequency-Shaped Robustness," *Journal of Guidance and Control,* Vol. 8, May-June 1985, pp. 397-401.

[3]Gupta, N. K., "Robust Control/Estimation Design by Frequency-Shaped Cost Functionals," *Proceedings of the 20th IEEE Conference on Decision and Control,* IEEE, New York, Dec. 1981, pp. 1167-1172.

[4]Johnson, T. L. and Athans, M., "On the Design of Optimal Constrained Dynamic Compensators for Linear Constant Systems," *IEEE Transactions on Automatic Control,* Vol. AC-15, Dec. 1970, pp. 658-660.

[5]Moerder, D. D. and Calise, A. J., "Convergence of a Numerical Algorithm for Calculating Optimal Output Feedback Gains," *IEEE Transactions on Automatic Control,* Vol. AC-30, Sept. 1985, pp. 900-903.

[6]Kramer, F. S. and Calise, A. J., "Fixed Order Dynamic Compensation for Multivariable Linear Systems," *Proceedings of the AIAA Guidance, Navigation, and Control Conference,* AIAA, New York, Aug. 1986, pp. 695-702.

[7]Bossi, J. A., "A Robust Compensator Design by Frequency Shaped Estimation," *Journal of Guidance and Control,* Vol. 8, July-Aug. 1985, pp. 541-544.

[8]Siciliano, B., Calise, A. J., and Jonnalagadda, V. R. P., "Optimal Output Fast Feedback in Two-Time Scale Control of Flexible Arms," *Proceedings of the 25th IEEE Conference on Decision and Control,* IEEE, New York, Dec. 1986.

Effects of Atmospheric Density Gradient on Control of Tethered Subsatellites

Junjiro Onoda* and Naoyuki Watanabe†
Institute of Space and Astronautical Science, Tokyo, Japan

Nomenclature

$[A]$, a_i	= plant matrix, see Eqs. (17), (21), and (24)
$[B]$	= input matrix, see Eqs. (17) and (22)
C_D	= aerodynamic drag coefficient
D	= aerodynamic drag force
$K_\delta, K_{\delta'}, K_\gamma, K_{\gamma'}$	= control gains, see Eq. (25)
l	= length of tether
m	= mass of subsatellite
$[Q]$	= weighting matrix of the state, see Eq. (26)
$\{q\}$	= state vector, see Eq. (18)
R	= radius of the orbit of main satellite
R_u	= weighting coefficient of the control force, see Eq. (26)
S	= equivalent drag area (involving both subsatellite and tether)
T	= tension in tether
t	= time
u	= normalized control force, see Eq. (23)
v	= velocity of subsatellite relative to the atmosphere
α	= angle between the local horizon and relative velocity vector, see Fig. 1
γ, δ	= normalized infinitesimal displacements of subsatellite from the steady-state equilibrium point, see Eqs. (19) and (20)
θ	= pitch angle between local vertical and tether line, see Fig. 1
λ	= coefficient of the atmospheric density gradient, see Eq. (16)
μ	= see Eq. (15)
ξ	= nondimensional length of tether, see Eq. (8)
ρ	= density of the atmosphere
τ	= nondimensional time, see Eq. (10)
Ω	= rotational angular rate of the Earth
ω	= orbital angular rate
Subscript	
s	= steady-state solution

I. Introduction

TETHERED subsatellites deployed in low-altitude orbits have been proposed as means of upper atmospheric experiments. Many works on the dynamics and control of the tethered subsatellites have been reported.[1] Beletskii and Levin[2] and Onoda and Watanabe[3] have shown that the atmospheric density gradient (together with the orbital angular velocity and the elasticity of the tether) unstabilizes the in-plane swinging motion of uncontrolled tethered subsatellites in the state of station keeping.

In this Note, the effects of the atmospheric density gradient on the swinging motion of tension-controlled tethered subsatellites and on the design of the control systems are investigated based on a simple model.

Received Jan. 12, 1988; revision received April 26, 1988.

*Associate Professor. Member AIAA.
†Research Associate.

II. Equations of Motion

Based on the same assumptions as Ref. 3, the equations of in-plane motion of the subsatellite can be written as follows in the orbit-fixed polar coordinates centered at the main satellite as shown in Fig. 1.

$$\xi'' + \{1 - [(\theta' + 1)^2 + 3\cos^2\theta]\}\xi = Q_l/(m\omega^2 l_s) \tag{1}$$

$$[\theta'' + (3/2)\sin 2\theta]\xi - 2(\theta' + 1)\xi' = Q_\theta/(m\omega^2 l_s^2 \xi) \tag{2}$$

$$Q_l = -T - D\sin(\alpha + \theta) \tag{3}$$

$$Q_\theta = -Dl_s\xi\cos(\alpha + \theta) \tag{4}$$

$$D = (1/2)\rho C_D S v^2 \tag{5}$$

$$v^2 = (\omega - \Omega)^2 R^2 + 2\omega(\omega - \Omega)Rl_s(\xi'\sin\theta + \xi\theta'\cos\theta) + \omega^2 l_s^2(\xi'^2 + \xi^2\theta'^2) \tag{6}$$

$$\sin\alpha = \omega l_s(\xi'\cos\theta - \xi\theta'\sin\theta)/v \tag{7}$$

where

$$\xi \equiv l/l_s \tag{8}$$

$$(\,)' \equiv \frac{\partial(\,)}{\partial\tau} \tag{9}$$

$$\tau \equiv \omega t \tag{10}$$

and

$$l/R \ll 1 \tag{11}$$

has been assumed and neglected compared with unity.

The steady-state solutions of Eqs. (1-7) can be obtained as

$$\xi_s = 1 \tag{12}$$

$$\theta_s = -\sin^{-1}[\mu R(1 - \Omega/\omega)/(3l_s)], \quad (\pi \le \theta_s \le 3\pi/2) \tag{13}$$

$$T_s = m\omega^2 l_s\{3\cos^2\theta_s + [\mu R(1 - \Omega/\omega)]^2/(3l_s^2)\} \tag{14}$$

where

$$\mu \equiv \rho_s C_D S R(1 - \Omega/\omega)/(2m) \tag{15}$$

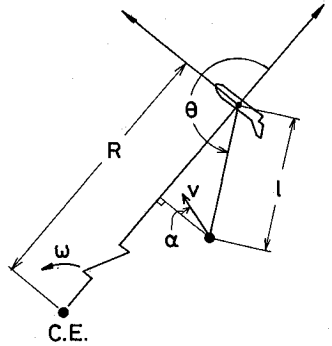

Fig. 1 Geometry of tethered subsatellite system.

and the atmospheric density has been assumed as

$$\rho = \rho_s \exp[-\lambda l_s(\xi\cos\theta - \xi_s\cos\theta_s)] \tag{16}$$

In this Note, it is also assumed that the control is available only through the modulation of tether tension. Then, in the case of linear control, the linearized equation of motion of small perturbation from the steady-state solution is

$$\{q\}' = [A]\{q\} + [B]u \tag{17}$$

where

$$\{q\}^T \equiv \lfloor \gamma, \gamma', \delta, \delta' \rfloor \tag{18}$$

$$\gamma = \xi - 1 \tag{19}$$

$$\delta = \theta - \theta_s \tag{20}$$

$$[A] = \begin{bmatrix} 0 & 1 & 0 & 0 \\ a_1 & a_2 & a_3 & a_4 \\ 0 & 0 & 0 & 1 \\ a_5 & a_6 & a_7 & a_8 \end{bmatrix} \tag{21}$$

$$[B]^T = \lfloor 0,1,0,0 \rfloor \tag{22}$$

$$u \equiv (T - T_s)/(m\omega^2 l_s) \tag{23}$$

and

$$a_1 = 3\cos^2\theta_s + (\mu/2)R(1 - \Omega/\omega)\lambda\sin 2\theta_s$$

$$a_2 = -\mu(1 + \sin^2\theta_s)$$

$$a_3 = [6\sin\theta_s + \mu R(1 - \Omega/\omega)/l_s]\cos\theta_s + \mu R(1 - \Omega/\omega)\lambda\sin^2\theta_s$$

$$a_4 = -2 + (\mu/2)\sin 2\theta_s$$

$$a_5 = 3\sin 2\theta_s + \mu[R(1 - \Omega/\omega)l_s]\cos\theta_s - \mu R(1 - \Omega/\omega)\lambda\cos^2\theta_s$$

$$a_6 = 2 + (\mu/2)\sin 2\theta_s$$

$$a_7 = -3\cos 2\theta_s + \mu[R(1 - \Omega/\omega)/l_s]\sin\theta_s - (\mu/2)R(1 - \Omega/\omega)\lambda\sin 2\theta_s$$

$$a_8 = -\mu(1 + \cos^2\theta_s) \tag{24}$$

$$u = -\lfloor K_\gamma, K_\gamma', K_\delta, K_\delta' \rfloor \{q\} \tag{25}$$

III. Numerical Examples and Discussions

In the subsequent numerical examples, the parameter values listed in Table 1 are used. They are the same as those of Ref. 3, and cases C-F roughly correspond to a subsatellite deployed in the altitude of 115 km with the projected drag area of 10 m^2 (including the effective area of the lowest portion of tether) and subsatellite mass of 500 kg.

Table 1 Control gains and eigenvalues of closed-loop systems ($R = 6.6 \times 10^6$ m, $l_s = 10^5$ m, $\omega = 1.18 \times 10^{-3}$ s^{-1}, $\Omega = 7 \times 10^{-5}$ s^{-1})

	Case A	Case B	Case C	Case D	Case E	Case F
μ	0.0	6.2×10^{-3}	6.2×10^{-3}	6.2×10^{-3}	6.2×10^{-3}	6.2×10^{-3}
λ (m^{-1})	–	0.0	1.5×10^{-4}	1.5×10^{-4}	1.5×10^{-4}	1.5×10^{-4}
K_γ	7.359	7.359	7.359	21.946	6.000	6.000
K_γ'	5.638	5.638	5.638	6.765	3.464	6.928
K_δ	3.070	3.070	3.070	8.407	0.0	0.0
K_δ'	1.767	1.767	1.767	−2.007	0.0	0.0
Nondimensional eigenvalues	$-1.017 \pm 1.963i$	$-0.976 \pm 1.964i$	$-2.609 \pm 2.435i$	$-1.311 \pm 2.530i$	$0.166 \pm 1.040i$	$-0.152 \pm 1.337i$
	$-1.046 + 0.0i$	$-1.142 + 0.0i$	$1.153 + 0.0i$	$-0.920 + 0.0i$	$-1.908 \pm 2.562i$	$-1.137 + 0.0i$
	$-2.558 + 0.0i$	$-2.565 + 0.0i$	$-0.556 + 0.0i$	$-3.243 + 0.0i$		$-5.507 + 0.0i$

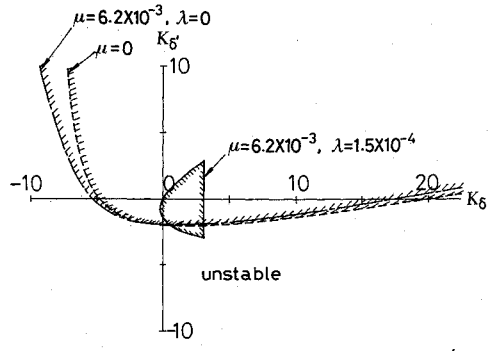

Fig. 2 Stable regions of controlled system in the K_δ–K_δ' plane ($R = 6.6 \times 10^6$ m, $l_s = 10^5$ m, $\omega = 1.18 \times 10^{-3}$ s^{-1}, $\Omega = 7 \times 10^{-5}$ s^{-1}, $K_\gamma = 7.359$, $K_\gamma' = 5.368$).

In the case of no atmosphere, i.e., $\mu = 0$, the optimal control gains that minimize

$$E(\{q\}^T[Q]\{q\} + R_u u^2) \tag{26}$$

for the linearized system is derived as case A of Table 1 based on the same weighting matrix as those used in Ref. 4, where $E(\ )$ denotes the expectation operator. The values obtained for the gains coincide with those of Ref. 4. When the values of two control gains K_γ and K_γ' are fixed to these values, the stable region in the $K_\delta - K_\delta'$ plane is obtained from Eqs. (17-25) and the Routh-Hurwitz's stability criterion as the upper region than the broken line of Fig. 2, which also coincides with the result of Ref. 4. For the case of $\mu = 6.2 \times 10^{-3}$, $\lambda = 0$, i.e., fictious case of locally uniform atmosphere, the stable region is obtained as the upper region than the one-dot chain line of Fig. 2. These two stable regions are similar to each other. However, in the case of $\mu = 6.2 \times 10^{-3}$ and $\lambda = 1.5 \times 10^{-4}$ m^{-1}, i.e., the realistic atmosphere with density gradient, the stable region is limited to the inside of the very small domain shown in Fig. 2 by the solid line. These facts indicate the significance of the effects of the atmospheric density gradient on the stability of controlled subsatellites.

The closed-loop eigenvalues are also listed in Table 1. They indicate that the system is stable in case A. Transient motions of the system obtained by a numerical integration of Eqs. (1-7) show well-controlled transient responses, although they are not shown here because of the need for brevity.

In case B of Table 1, the same gains as case A are adopted to the system with fictitious atmosphere whose density is locally uniform. The eigenvalues are almost the same as those of case A, and the system is stable. This fact indicates that the effects of the atmosphere are small if its density were uniform.

Case C is the case where the same gains as case A are adopted to the subsatellite deployed in the real atmosphere with density gradient. Unlike cases A and B, one of the real parts of the eigenvalues of case C is positive, indicating that the system is unstable. Reference 3 lists the eigenvalues of an uncontrolled subsatellite obtained, based on the same parameter values as case C, and a realistic longitudinal stiffness of the tether. It should be noted that the positive real part of an eigenvalue of case C, 1.153, is much larger than that of uncontrolled subsatellite, 3.517×10^{-2}, which can be obtained by normalizing the result of Ref. 3. This fact indicates that the effects of the density gradient can be far more significant for the controlled system than for the uncontrolled one, and a control system designed without any account of the atmospheric density gradient can make the system quite unstable. In Ref. 3, it has been suggested that lower longitudinal stiffness of the tether unstabilizes the system. Since the gain K_γ corresponds to the longitudinal stiffness, the previous relatively strong instability seems to be caused by the relatively small control gain K_γ.

The optimal linear quadratic Gaussian (LQG) control gains can be obtained based on the actual values of μ and λ, i.e., actual atmospheric parameters, as case D in Table 1. In this case, the eigenvalues indicate that the system is stable. As can be expected from the preceding investigation, the longitudinal stiffness K_γ is very large in this stable system. Transient responses, which are not shown in this Note because of lack of space, indicate that the system is relatively well controlled, although a relatively large control force suggests the difficulty of control in the atmospheric density gradient.

Case E and case F are the examples where the Rupp's control laws[5] are adopted. The former is the case of $\xi = 1$, and the latter is the case of $\xi = 2$ according to the notation of Ref. 5. The eigenvalues indicate that the motion is unstable in case E and stable in case F. The transient responses of case F, which are not shown here, indicate that the system is not as well controlled as is in case D although the closed-loop system of case F is stable.

IV. Concluding Remarks

The effects of the atmospheric density gradient on the in-plane motion of tension-controlled tethered subsatellites deployed in a low-altitude orbit are investigated, based on a simple model. It is shown that the effect on the stability of the controlled system can be more significant than on that of the uncontrolled system. A control system designed without any account of the atmospheric density gradient can greatly unstabilize the closed-loop system. Therefore, it is indispensible to consider the effects of the density gradient in the design of the control system of tethered subsatellites deployed in low-altitude orbits.

Although the present Note has clarified the effects of the atmospheric density gradient qualitatively based on the simplified model, further investigations with a more exact model are still required.

References

[1]Misra, A. K. and Modi, V. J., "A Survey on the Dynamics and Control of Tethered Satellite Systems," *Tethers in Space, Advances in the Astronautical Sciences*, Vol. 62, AAS Publications, 1987, pp. 667-720.

[2]Beletskii, V. V. and Levin, E., "Dynamics of the Orbital Cable System," *Acta Astronautica*, Vol. 12, 1985, pp. 285-291.

[3]Onoda, J. and Watanabe, N., "Tethered Subsatellite Swinging from Atmospheric Gradients," *Journal of Guidance, Control, and Dynamics* (to be published).

[4]Bainum, P. M. and Kumar, V. K., "Optimal Control of the Shuttle-Tethered-Subsatellite System," *Acta Astronautica*, Vol. 7, Dec. 1980, pp. 1333-1348.

[5]Rupp, C. C., "A Tether Tension Control Law for Tethered Subsatellite Deployed Along Local Vertical," NASA TMX-64963, Sept. 1975.

Optimal Terminal Maneuver for a Cooperative Impulsive Rendezvous

John E. Prussing* and Bruce A. Conway†
University of Illinois at Urbana-Champaign, Urbana, Illinois

I. Introduction

IN this Note, the optimal terminal maneuver is determined for a cooperative impulsive rendezvous of two space vehi-

Received Oct. 26, 1987; revision received March 29, 1988.

*Professor, Department of Aeronautical and Astronautical Engineering. Associate Fellow AIAA.

†Associate Professor, Department of Aeronautical and Astronautical Engineering. Associate Fellow AIAA.